Filtration properties of nanofiber/microfiber mixed filter and prediction of its performance

doi: 10.4209/aaqr.2016.06.0256

Filtration properties of nanofiber/microfiber mixed filter and prediction of its performance

Hyun-Jin Choi[1], Mikio Kumita[1*], Sho Hayashi[1], Hisashi Yuasa[1], Mie Kamiyama[2], Takafumi Seto[1], Chuen-Jinn Tsai[3], and Yoshio Otani[1]

[1] School of Natural System, College of Science and Engineering, Kanazawa University, Kakuma-machi, Kanazawa, Ishikawa 920-1192, Japan
[2] Teijin Limited, Minohara, Ibaraki, Osaka, 567-0006, Japan
[3] Institute of Environmental Engineering, National Chiao Tung University, University road, Hsinchu 30010, Taiwan

Abstract

There is an increasing demand of air filters with a high collection performance, i.e., high collection efficiency and low pressure drop, for the application to indoor air cleaning. Air filters consisting of nanofibers have attracted great interests since they may have a low pressure drop because of slip flow effect and high collection efficiency due to interception. Although various nanofiber filters are available on the market, their collection performance is not as high as expected by the conventional filtration theory because non-uniform packing of fibers plays a significant role. In the present work, the collection performance of nanofiber (780 nm) and microfiber (11.2 μm) mixed filters with various mixing fractions was studied in order to maximize the quality factor of filter, q_F, as a function of mixing fraction of nanofibers. The collection performance of mixed fiber filters was predicted by using theoretical equations reported by Bao *et al*. (1998) for bimodal distribution of fibers. As a result, it was found that the mixed fiber filters had a uniform fiber packing compared to laminated filters and that the collection efficiency was well predicted by introducing the inhomogeneity factor calculated for the filter consisting of two distinct fiber sizes. Furthermore, we found that the mixed fiber filter with the nanofiber mixing fraction of 5% in mass had the highest quality factor.

Keywords: Air filtration, Mixed fiber filter, Mixing fraction, Quality factor, Inhomogeneity factor

*Corresponding author. Tel: 81-76-234-4827; Fax: 81-76-234-4826
E-mail address: kumita@se.kanazawa-u.ac.jp

INTRODUCTION

Recent progress in manufacturing technology of polymer fibers enables us to produce nanofibers in large quantity at a relatively low cost. Air filters made of nanofibers with the diameter less than 1 μm have attracted great attention because they may attain a high collection efficiency with a low pressure drop at the same time. Various manufacturing methods, e.g., melt-blown, electrospinning and stretching of polymer films, have been developed to obtain fine fibers (Uppal *et al*., 2013; Cho *et al*., 2013; Hassan *et al*., 2013). Especially, electrospinning is the most popular method because it is simple and is able to fabricate nanofibers of various polymers (Choi *et al*., 2014). Maze *et al*. (2007) studied the collection efficiency of nanofiber filters laminated on a base filter using a theoretical 3-D model, and showed that the reduction in fiber diameter was effective for increasing the collection efficiency. Matulevicius *et al*. (2014) experimentally measured the collection performance of nanofiber filter media fabricated by electrospinning of polyamide, and reported that the filter with finer fibers had a high collection efficiency and a high quality factor. Sambaer *et al*. (2014) and Podgorski *et al*. (2011) introduced the inhomogeneity factor in the prediction of collection efficiency of a laminated nanofiber filter, which was originally proposed by Kirsch *et al*. (1975), and reported that the predicted collection efficiency agreed well with the experimental data by the correction with the inhomogeneity factor. They also reported that the inhomogeneity factor of nanofiber filter was high compared to HEPA filters.

Since nanofiber layers are usually membrane-like thin film, they are not uniform in packing and have a low mechanical strength. They also have a relatively high packing density, resulting in a high initial pressure drop and rapid clogging by the deposited particles (Leung *et al*., 2008). In order to resolve these issues, nanofiber layers with a unique property such as multi-layered filters, beaded nanofibers and sphere-nanofiber mixed filters have been proposed (Yun *et al*., 2010; Hung and Leung, 2011; Mei *et al*., 2013; Ogi *et al*., 2014). However, in these previous works, the packing densities of nanofiber filters were not low enough so that the pressure drop was relatively high and the dust holding capacity was low.

In the present work, the collection performance of nanofiber/microfiber composite filters was studied, in which nanofibers are well dispersed among micrometer fibers. Nanofiber/microfiber mixed filters are expected to resolve the problems of laminated filters, such as low mechanical strength, non-uniform packing of fibers as well as the short service life. In this study, the nanofiber/microfiber mixed filters with various mixed fractions of nanofibers were prepared by a liquid filtration of nanofiber/microfiber suspensions, and the collection performance was evaluated experimentally. In the prediction of collection performance of mixed fiber filters, we applied the theoretical equation for a filter with a bimodal fiber diameter distribution reported by Bao *et al*. (1998). We also attempted to optimize the mixing fraction of nanofiber based on the quality factor.

FILTRATION THEORY OF AIR FILTER

The mechanical collection mechanisms of air filters are Brownian diffusion, inertia, interception, and gravity. The relative contribution of each collection mechanism to the particle collection depends upon the physical properties of filter (fiber diameter, packing density, orientation of fibers and internal structure of filter), and particle properties (particle diameter, particle density, and the shape) as well as the filtration conditions (filtration velocity, pressure, and temperature) (Hinds, 1999).

HEPA filters composed of submicron fibers (E > 99.97% for 0.3-μm particles) remove particles mainly by Brownian diffusion and interception, and the collection efficiency is affected

by the internal structure of filter, such as the variance of fiber diameter, the inhomogeneity factor, and the packing density. Kirsch and Stechkina (1978) proposed the prediction method of HEPA filter based on the single fiber efficiency of Fan Model Filter (FMF) due to Brownian diffusion and interception. FMF is the filter in which monodispersed fibers are randomly packed and all of the fibers are placed perpendicular to the air flow. Since the inhomogeneity factor is defined as the ratio of pressure drop of FMF to that of a real filter at $Kn = 0$, non-uniformity of fiber diameter, inclination of fibers to airflow, uneven packing of fibers determine the inhomogeneity factor. Moreover, the slip flow effect on fiber surfaces becomes significant as the fiber size decreases. The single fiber collection efficiency of FMF accounting for the influence of slip flow is given by the following equations:

$$\eta_{\mathrm{T}}^{\mathrm{f}} = \eta_{\mathrm{D}} + \eta_{\mathrm{R}} + \eta_{\mathrm{DR}} \tag{1}$$

$$\eta_{\mathrm{D}} = 2.7 Pe^{-2/3} \left\{ 1 + 0.39 \left(K^{\mathrm{f}} \right)^{-1/3} Pe^{1/3} Kn \right\} \tag{2}$$

$$\eta_{\mathrm{R}} = \frac{1}{2K^{\mathrm{f}}} \left\{ 2(1+R)\ln(1+R) - (1+R) + \frac{1}{1+R} + 2.86 Kn \frac{(2+R)R}{1+R} \right\} \tag{3}$$

$$\eta_{\mathrm{DR}} = 1.24 \left(K^{\mathrm{f}} \right)^{-1/2} Pe^{-1/2} R^{2/3} \tag{4}$$

where $\eta_{\mathrm{T}}^{\mathrm{f}}$ is the single fiber collection efficiency of FMF, η_{D} and η_{R} are the diffusion and interception single fiber collection efficiencies, η_{DR} is the interaction term for diffusion and interception. Pe is the Peclet number defined by Eq. (5), R is the interception parameter given by Eq. (6), Kn is the Knudsen number, defined by Eq. (7), and K^{f} is the hydrodynamic factor with the correction for slip flow given by Eq.(8):

$$Pe = \frac{u d_{\mathrm{f}}}{D} \tag{5}$$

$$R = \frac{d_{\mathrm{p}}}{d_{\mathrm{f}}} \tag{6}$$

$$Kn = \frac{2\lambda}{d_{\mathrm{f}}} \tag{7}$$

$$K^{\mathrm{f}} = -0.5 \ln \alpha - 0.52 + 0.64\alpha + 1.43(1-\alpha) Kn \tag{8}$$

where, u is the filtration velocity (here, we define it as the interstitial velocity), d_{f} the fiber diameter, D the diffusivity of particles, d_{p} the particle diameter, λ the mean free path of air molecules, α the packing density of filter. For the prediction of collection efficiency of real fiber, Kirsch and Stechkina (1978) introduced the variance of fiber diameter, σ, and the inhomogeneity factor, δ. σ and δ are given by the following equations when the fiber size distribution follows a lognormal distribution.

$$\sigma = \frac{\overline{d_{\mathrm{f}}^2} - \overline{d}_{\mathrm{f}}^2}{\overline{d}_{\mathrm{f}}^2} = \exp\left(\ln \sigma_{\mathrm{g}} \right)^2 - 1 \tag{9}$$

$$d_{\mathrm{f}} = \overline{d}_{\mathrm{f}} = d_{\mathrm{fg}} \exp\left\{ 0.5 \left(\ln \sigma_{\mathrm{g}} \right)^2 \right\} \tag{10}$$

$$\delta = \left(\frac{\Delta p^{\mathrm{f}}}{\Delta p^{\mathrm{r}}} \right)_{Kn=0} \tag{11}$$

where d_{fg} is the geometric mean diameter of fiber, σ_g the geometric standard deviation, and the superscripts f and r denote respectively "FMF" and "real".

Because the total fiber length per unit filter volume is $l = \alpha L \Big/ \left\{ (\pi/4) \overline{d_f^2} \right\}$ and $\overline{d_f^2} = (1+\sigma)\bar{d}_f^2$ from Eq. (9), the packing density, α, which appears in Eq. (8), should be replaced by $\alpha/(1+\sigma)$.

The filter efficiency, *E*, is related to the single fiber collection efficiency of FMF by the following Eq. (12):

$$E = 1 - P = 1 - \exp\left\{ -\frac{4}{\pi} \frac{\alpha}{(1-\alpha)(1+\sigma)} \frac{L}{\bar{d}_f} \frac{\eta_T^f}{\delta} \right\} \tag{12}$$

EXPERIMENTAL SETUP AND METHOD

Test Filters

Nanofibers ($d_f = 780$ nm) used in this study were produced from a sea-island type PET/co-PET conjugal fibers. This type of nanofibers has a uniform fiber diameter compared to that prepared by the other methods. The nanofibers were dispersed in water with the aid of a surfactant together with monodisperse 11.2-μm PET fibers. The packing densities of nanofibers and microfibers in the mixed fiber filter cannot be measured after the fabrication of mixed fiber filters. Therefore, when preparing the suspension of mixed fibers, we mixed a known mass of nanofibers, M_N, and a known mass of microfibers, M_M, into the suspension and filtrate all of the suspension to form a filter sheet. Therefore, we know the exact masses of nanofibers and microfibers in the prepared filter so that we can determine the mixing fraction of nanofibers in the prepared filter sheet:

$$MF = \frac{M_N}{M_N + M_M} \tag{13}$$

Test filters were prepared at the mixing fractions of *MF* = 5, 10, 20, and 30%. The structure of the prepared filter was examined using a scanning electron microscope (SEM, JSM 6390AX, JEOL). The packing density of test filter was calculated by the following equation:

$$\alpha = \frac{W}{L\rho} \tag{14}$$

where ρ is the density of fibers (for PET, 1400 kg m^{-3}), *L* the filter thickness measured by a micrometer, and *W* the filter area density. The packing densities of nanofibers and microfibers, α_N and α_M, were calculated by the following equations:

$$\alpha_N = MF \cdot \alpha \tag{15}$$

$$\alpha_M = (1 - MF)\alpha \tag{16}$$

Measurement of filtration performance

Experimental setup for measuring the particle penetration and pressure drop is shown in Fig. 1. In this study, particles with diameters ranging from 10 nm to 7 μm were used to determine the particle penetration. Monodispersed NaCl particles with equilibrium charge ranging from 10 to 200 nm in diameter were generated by an evaporation/condensation method using a tubular electric furnace, differential mobility analyzer (DMA, Model 3081, TSI) and a neutralizer

(^{241}Am). Condensation Particle Counter (CPC, Model 3775, TSI) was used for measuring the particle number concentration upstream and downstream of the filter. Standard test powder JIS-11 (SP3-3, Association of Powder Process Industry and Engineering, Japan) was used for determining particle penetration in the size range from 300 nm to 7 μm. Polydispersed JIS-11 particles were generated by a fluidized bed dust generator (Model 3080, Kanomax Inc.) and neutralized using an ^{241}Am neutralizer. Optical Particle Sizer (OPS, Model 3330, TSI) was used for measuring the particle concentration. Filtration velocity was varied from 5 to 10 cm s^{-1}. The penetration, P, was calculated by the following equation:

$$P = \frac{C_{\text{out}}}{C_{\text{in}}} \tag{17}$$

where C_{out} is the particle concentration downstream of the filter and C_{in} is the upstream concentration. The pressure drop was measured by a differential monometer (Testo 510, Testo AG) at filtration velocity, u = 0, 5, 10, 15 and 20 cm s^{-1}.

RESULTS AND DISCUSSION

Physical properties of prepared filters

Table 1 shows the physical properties of the test filters. Other than the filter with the mixing fraction of nanofibers 5%, the filters prepared at the mixing fractions above 10% have almost the same thickness of 237 μm. The area density and the packing density increase with the mixing fraction. Fig. 2 shows the cross-sectional views of filters prepared at various mixing fractions. As seen in the figure, there exist a few bundles of nanofibers but the nanofibers are fairly well dispersed uniformly among the microfibers in the filter matrix.

Filtration performance

The penetrations through the test filters at filtration velocity of 5 cm s^{-1} are shown in Fig. 3(a) and those at 10 cm s^{-1} in Fig. 3(b). It is seen from these figures that the particle penetration decreases with increasing the nanofiber mixing fraction, and the MPPS (Most Penetrating Particle Size) shifts toward to smaller particle size with increasing the mixing fraction. This is because the collection of particles with nanofibers becomes more significant with increasing the mixing fraction of nanofibers. Choi *et al*. (2014) reported that the interception is a predominant collection mechanism in nanofiber filtration even for ultrafine particles, and its contribution increases with decreasing fiber diameter. Leung *et al*. (2010) also reported that the coating of nanofiber on a substrate enhances the filtration efficiency and reduces the MPPS down to a smaller size of particles. The penetration of 300 nm particles at *MF* = 30% is 99.95% at the filtration velocity of 5 cm s^{-1}, which is close to the collection efficiency of HEPA filters. The penetrations of particles smaller than the MPPS at the filtration velocity of 10 cm s^{-1} are higher than those at 5 cm s^{-1}, while the penetrations of particles larger than the MPPS are almost the same as those of at 5 cm s^{-1}. The dependence of penetration on filtration velocity proves that, for the present nanofiber/microfiber composite filters with all maxing fractions, Brownian diffusion is the dominant collection mechanism for particles smaller than the MPPS while that the interception is predominant for particles larger than the MPPS.

Fig. 4 shows the pressure drop of test filters as a function of mixing fraction. The pressure drop increases with the mixing fraction, however the relationship between the pressure drop and the mixing fraction is not linear. As shown in the figure, the increase in pressure drop up to 20% mixing fraction is not so significant, but the pressure drop increase from *MF* = 20% to 30% is abrupt. As shown in Fig. 2, the individual nanofibers are well dispersed in the filter matrix at the

mixing fractions of 5% and 10%, but the amount of nanofibers is not so large to change the pressure drop significantly. However, when *MF* = 30%, we see many bundles of nanofibers but there exist many individually dispersed nanofibers. Consequently, small increase in pressure drop up to 20% may be attributed to the small contribution of nanofibers on the pressure drop, and the abrupt increase in pressure drop from 20% to 30% may result from the increased number of individual nanofibers in the filter matrix although there are many bundles of nanofibers.

Prediction of filtration performance of mixed fiber filters

In this study, the test filters are composed of monodisperse fibers with two distinct diameters, and therefore the fiber diameter distribution is not expressed by a lognormal distribution function. Bao *et al*. (1998) proposed a prediction method of the pressure drop and penetration of a HEPA filter which consisted of mixed fibers with two different average sizes. In predicting the penetration and pressure drop of the nano/microfiber mixed filter, we applied their prediction method by setting the variances of nanofibers and microfibers equal to zero. In their prediction, they assumed that the nanofibers and microfibers independently contributed to the pressure drop of mixed fiber filters. Therefore, we may estimate the pressure drop of our composite filters by adding the pressure drops of nanofibers and microfibers. The theoretical pressure drop of composite filter, Δp^{f}, is given by the following equations:

$$\Delta p^{\mathrm{f}} = \Delta p_{\mathrm{N}}^{\mathrm{f}} + \Delta p_{\mathrm{M}}^{\mathrm{f}} = F^{\mathrm{f}} u \mu l_{\mathrm{N}} + F^{\mathrm{f}} u \mu l_{\mathrm{M}} \tag{18}$$

$$F^{\mathrm{f}} = \frac{4\pi}{K^{\mathrm{f}}} \tag{19}$$

$$l_{\mathrm{N}} = \frac{4\alpha_{\mathrm{N}} L}{\pi d_{\mathrm{fN}}^2} \tag{20}$$

$$l_{\mathrm{M}} = \frac{4\alpha_{\mathrm{M}} L}{\pi d_{\mathrm{fM}}^2} \tag{21}$$

where the subscripts N and M refer to the nanofiber and microfiber, l is the fiber length in unit filter area. F^{f} is the dimensionless drag, and μ is the viscosity of air.

Fig. 5 compares the experimental pressure drops and the theoretical ones for the mixed fiber filters as a function of filtration velocity. The symbols and the lines represent the measured pressure drop and the predicted pressure drop, respectively. As seen in this figure, the experimental pressure drops are in fairly good agreement except the mixing fraction of 5% and 20%. The discrepancy between the predicted and the experimental data represent the degree of inhomogeneity of fibers, which was introduced by Kirsch *et al*. (1975) for accounting the inhomogeneous packing of fibers and the orientation of fibers in filter media in predicting the collection efficiency of a filter. For mixed fiber filters we introduced the inhomogeneity factor which is the ratio of theoretical pressure drop predicted by Eqs. (18) – (21) over the measured pressure drop. Table 2 shows the inhomogeneity factors in the far right column. In all mixing fractions, the inhomogeneity factors are smaller than 3.3, and the maximum value among four tested filters is 3.27 at the mixing fraction of 20%. The table also shows the contributions of nanofibers to the pressure drop of mixed fiber filters. Even for the mixed fiber filter with the mixing fraction of 5%, the contribution of nanofibers is 74.4% on the total pressure drop, implying that the addition of nanofibers drastically changes the pressure drop even when the mass fraction is small.

The penetration of the nanofiber/microfiber mixed filters is given by the following equation:

$$\ln P = \ln P_{\mathrm{N}} + \ln P_{\mathrm{M}} \tag{22}$$

$$\ln P_N = -d_{fN}\eta_{TN}l_N/\delta \quad (23)$$

$$\ln P_M = -d_{fM}\eta_{TM}l_M/\delta \quad (24)$$

Figs. 6 and 7 show the comparison of predicted penetrations of mixed filters with the experimental ones at the filtration velocities of 5 and 10 cm s^{-1}. The solid lines are the theoretical penetrations of mixed fiber filters and the broken and dotted lines are the penetrations of nanofibers and microfibers, respectively. As shown in the figures, the predicted penetrations are in good agreement with the experimental data, indicating that theory of the bimodal fiber diameter distributions with the correction by inhomogeneity factor is an effective means for predicting the penetration of the nano/microfiber mixed filters. This prediction also revealed that the contribution of nanofiber for particle collection is essential even if the mixing fraction is 5%. Since the contribution of the nanofibers to the pressure drop was 74.4% at the mixing fraction of 5% in Table 2, it may be said, that the addition of nanofibers to air filters affects the collection efficiency more than the pressure drop.

Filter quality factor is a useful parameter to compare the filtration performance of various filter media. It is defined by the following equation (Hinds, 1999):

$$q_F = -\ln P/\Delta p \quad (25)$$

We can calculate the theoretical quality factor of mixed fiber filter, q_F^f, for FMF by substituting Eqs. (18) and (22)–(24) by setting $\delta = 1$:

$$q_F^f = \frac{d_{fN}\eta_{TN}^f l_N + d_{fM}\eta_{TM}^f l_M}{F^f u\mu l_N + F^f u\mu l_M} \quad (26)$$

Fig. 8 shows the predicted filter quality factor of mixed filters as a function of mixing fraction of nanofibers, respectively at u = 5, 10 cm s^{-1} together with the experimental data. Although the quantitative agreement between the experimental data and prediction is fair, the predicted maximal value of quality factors are in agreement with the experimental data, appearing at around mixing fraction of 5% for all particle diameters and both filtration velocities.

The optimal values of mixing fraction of nanofiber can be obtained by partially differentiating Eq. (26) with respect to packing density of nanofiber and setting it equal to zero for an arbitrary combination of nanofibers and microfibers at various packing densities of fibers. Fig. 9 shows the maximum quality factor by the solid line and the mixing fraction of nanofiber which gives the maximum quality factor by the broken line, as a function of packing density of filter media. As seen in the figure, the maximal quality factor increases with decreasing the packing density of filter media, and the mixing fraction of nanofiber which gives the maximum in quality factor becomes smaller with decreasing the packing density. What follows from the prediction of performance of nanofiber/microfiber mixed fiber filter is that the quality factor increases by reducing the mixing fraction of nanofiber in microfiber filter media with a small packing density.

In Fig. 9, the nanofiber diameter was 780 nm, which was fairly large in diameter to be called as a nanofiber. If we could reduce the nanofiber diameter in the mixed fiber filter, the influence of packing density on the maximal quality factor would be different. Fig. 10 shows the predicted maximum quality factors and the mixing fraction of nanofiber which gives the maximum quality factor as a function of packing density of filter media when 100 nm nanofibers are mixed with 11.2 μm microfibers. As seen in the figure, the maximal value of quality factor for d_{fN} = 100 nm is almost doubled compared to that for d_{fN} = 780 nm (Fig. 9), and the dependence of quality factor on the packing density is less pronounced. The mixing fraction of nanofiber which gives the maximum quality factor ranges from 0.3 to 1.5%. Consequently, if we employ finer nanofiber we may make nanofiber/microfiber mixed filter with a high quality factor in a wide range of packing density.

CONCLUSION

The performance of a nano/microfiber composite filter was investigated both theoretically and experimentally from viewpoint of the quality factor. In case of mixed fiber filter consisting of 780 nm and 11.2 μm fibers with various mass factions at the packing density of 0.18, the maximum value of quality factor appears at 5% of mass fraction of nanofibers, which was confirmed experimentally and theoretically. The prediction method of quality factor for the nano/microfiber mixed filters proposed in the present work enables the estimations of maximum quality factor and optimal mixing fraction of nanofibers for various combinations of nano/microfiber diameters at a given packing density of filter media.

REFERENCES

Bao, L., Otani, Y., Namiki, N., Mori, J., and Emi, H. (1998). Prediction of HEPA filter collection efficiency with a bimodal fiber size distribution. *Kagaku Kogaku Ronbunshu*, 24:766-771.

Cho, D., Naydich, A., Frey, M. W., and Joo, Y. L. (2013). Further improvement of air filtration efficiency of cellulose filters coated with nanofibers via inclusion of electrostatically active nanoparticles. *Polymer*, 54:2364-2372.

Choi, H. -J., Kim, S. B., Kim, S. H., and Lee, M. –H. (2014). Preparation of electrospun polyurethane filter media and their collection mechanisms for ultrafine particles. *J. Air Waste Manage. Assoc*., 64:322-329.

Hassan, M. A., Yeom. B. Y., Wilkie, A., Pourdeyhimi, B., and Khan, S. A. (2013). Fabrication of nanofiber meltblown membranes and their filtration properties. *J. Membr. Sci*., 427:336-344.

Hinds, W. C., (1999). *Aerosol Technology: Properties, Behavior, and Measurement of Airborne Particles*, 2nd ed., Wiley, New York.

Hung, C. –H., and Leung. W. W. –F. (2008). Investigation on pressure drop evolution of fibrous filter operating in aerodynamic slip regime under continuous loading of sub-micron aerosols. *Sep. Purif. Technol*., 63:691-700.

Kirsch, A. A., Stechkina, I. B., and Fuchs N. A. (1975). Efficiency of aerosol filters made of ultrafine polydisperse fibers. *J. Aerosol Sci*., 6:119-120.

Kirsch, A. A., and Stechkina, I. B. (1978). The theory of aerosol filtration with fibrous filters. *In Fundamentals of Aerosol Science*. ed. D. T. Shaw, John Wiley&Sons, New York.

Leung, W. W. -F., Hung, C. -H., and Yuen, P. T. (2009). Experimental Investigation on continuous filtration of sub-micron aerosol by filter composed of dual-layers including a nanofiber layer. *Aerosol Sci Tecnol*., 43:1174-1183.

Leung, W. W. -F., Hung, C. -H., and Yuen, P. T. (2010). Effect of face velocity, nanofiber packing density and thickness on filtration performance of filters with nanofibers coated on a substrate. *Sep. Purif. Technol*., 71:30-37.

Matulevicius, J., Kliucininkas, L., Martuzevicius, D., Krugly, E., Tichonovaas, M. and Baltrusaitis, J. (2014). Design and Characterization of Electrospun Polyamide Nanofiber media for Air Filtration Applications. *J. Nanomaterials.* Article ID:859656.

Maze, B., Tafreshi, H. V., Wang, Q., and Pourdeyhimi, B. (2007). A Simulation of un-steady-state filtration via nanofiber media at reduced operating pressures. *J. Aerosol Sci.* 38: 550-571.

Mei, Y., Wang, Z., and Li, X. (2012). Improving filtration performance of electrospun nanofiber mats by a bimodal method. *J. Appl. Polym. Sci*., 128:1089-1094.

Ogi, T., Ono, H., Bao, L., Niinima, H., and Okuyama, K. (2014). Morphology-controlled synthesis of electron nanofibers and their application for aerosol filtration. *Kagaku Kogaku Ronbunshu*. 40: 84-89.
Podgorski, A., Maisser, A., Szymanski, W. W., Jackiewicz, A., and Gradon, L. (2011). Penetration of monodisperse, singly charged nanoparticles through polydisperse fibrous filters. *Aerosol Sci Tecnol.* 45: 215-233.
Sambaer, W., Zatloukai, M., and Kimmer, D. (2011). 3D modeling of filtration process via polyurethane nanofiber based nonwoven filters prepared by electrospinning process. *Chem. Eng. Sci*., 66:613-623.
Uppal. R., Bhat, G., Eash. C., and Akato, K. (2013). Meltblown nanofiber media for enhanced quality factor. *Fibers and Polymers*, 14: 660-668.
Yun, K. M., Suryamas, A. B., Iskandar, F., Bao, L., Niinuma, H., and Okuyama, K. (2010). Morphology optimization of polymer nanofiber for applications in aerosol particle filtration. *Sep. Purif. Technol*., 75:340-345.

Table Titles

Table 1. Physical properties of the nanofiber/microfiber mixed filters.

Table 2. Contribution ratio and inhomogeneity factor of the nanofiber/microfiber mixed filters.

Table 1. Physical properties of the nanofiber/microfiber mixed filters.

Mixing fraction MF [%]	Microfiber diameter, d_{fM} [μm]	Nanofiber diameter, d_{fN} [nm]	Thickness, L [μm]	Area density, W [g m^{-2}]	Packing density, α [-]
5	11.2	780	276 ± 32	57.2	0.152
10	11.2	780	237 ± 47	58.4	0.172
20	11.2	780	235 ± 35	59.8	0.186
30	11.2	780	239 ± 20	62.2	0.195

Table 2. Contribution ratio and inhomogeneity factor of the nanofiber/microfiber mixed filters.

Mixing fraction *MF* [%]	Contribution of nanofibers on total pressure drop [%]		δ [-]
	Nanofibers	Microfibers	
5	74.4	25.6	3.20
10	87.7	12.3	2.68
20	95.5	4.5	3.27
30	97.9	2.1	1.57

Figure Captions

Fig. 1. Experimental setup for determining particle collection efficiency and pressure drop.
Fig. 2. Cross-sectional morphologies of the nanofiber/microfiber mixed filters.
Fig. 3. Particle penetration through the nanofiber/microfiber mixed filter, (a) u = 5 cm s^{-1} (b) u = 10 cm s^{-1}.
Fig. 4. Pressure drop of the nanofiber/microfiber mixed filter as a function of mixing fractions.
Fig. 5. Comparison of theoretical pressure drops and experimental pressure drops.
Fig. 6. Theoretical and experimental particle penetration of the nanofiber/microfiber mixed filters at u = 5 cm s^{-1}.
Fig. 7. Theoretical and experimental particle penetration of the nanofiber/microfiber mixed filters at u = 10 cm s^{-1}.
Fig. 8. Quality factor of the nanofiber/microfiber mixed filter as a function of mixing fractions.
Fig. 9. Maximum quality factor and the mixing fraction of nanofiber (d_{fN} = 780 nm) which gives the maximum quality factor as a function of packing density of filter media.
Fig. 10. Maximum quality factor and the mixing fraction of nanofiber (d_{fN} = 100 nm) which gives the maximum quality factor as a function of packing density of filter media.

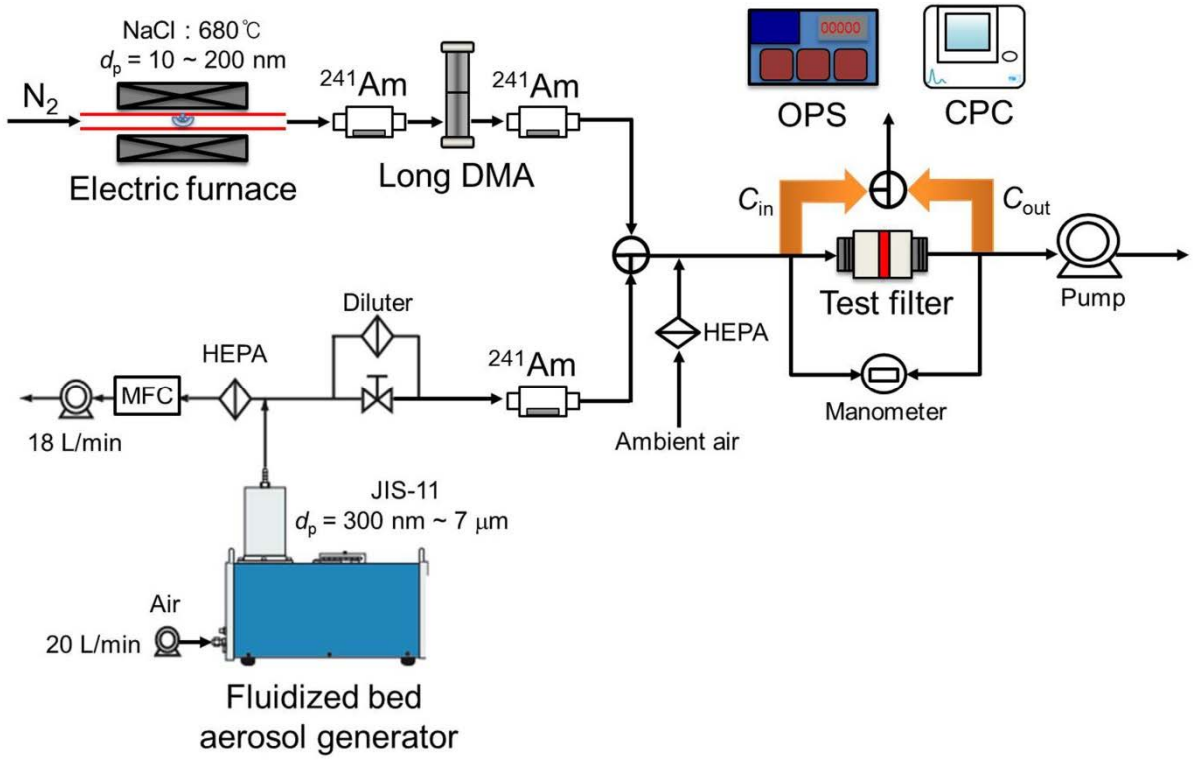
NaCl : 680℃
d_p = 10 ~ 200 nm
N_2
Electric furnace
^{241}Am
Long DMA
^{241}Am
OPS
CPC
C_{in}
C_{out}
Test filter
Pump
Manometer
HEPA
Ambient air
Diluter
HEPA
MFC
18 L/min
^{241}Am
JIS-11
d_p = 300 nm ~ 7 μm
Air
20 L/min
Fluidized bed
aerosol generator

Figure 1

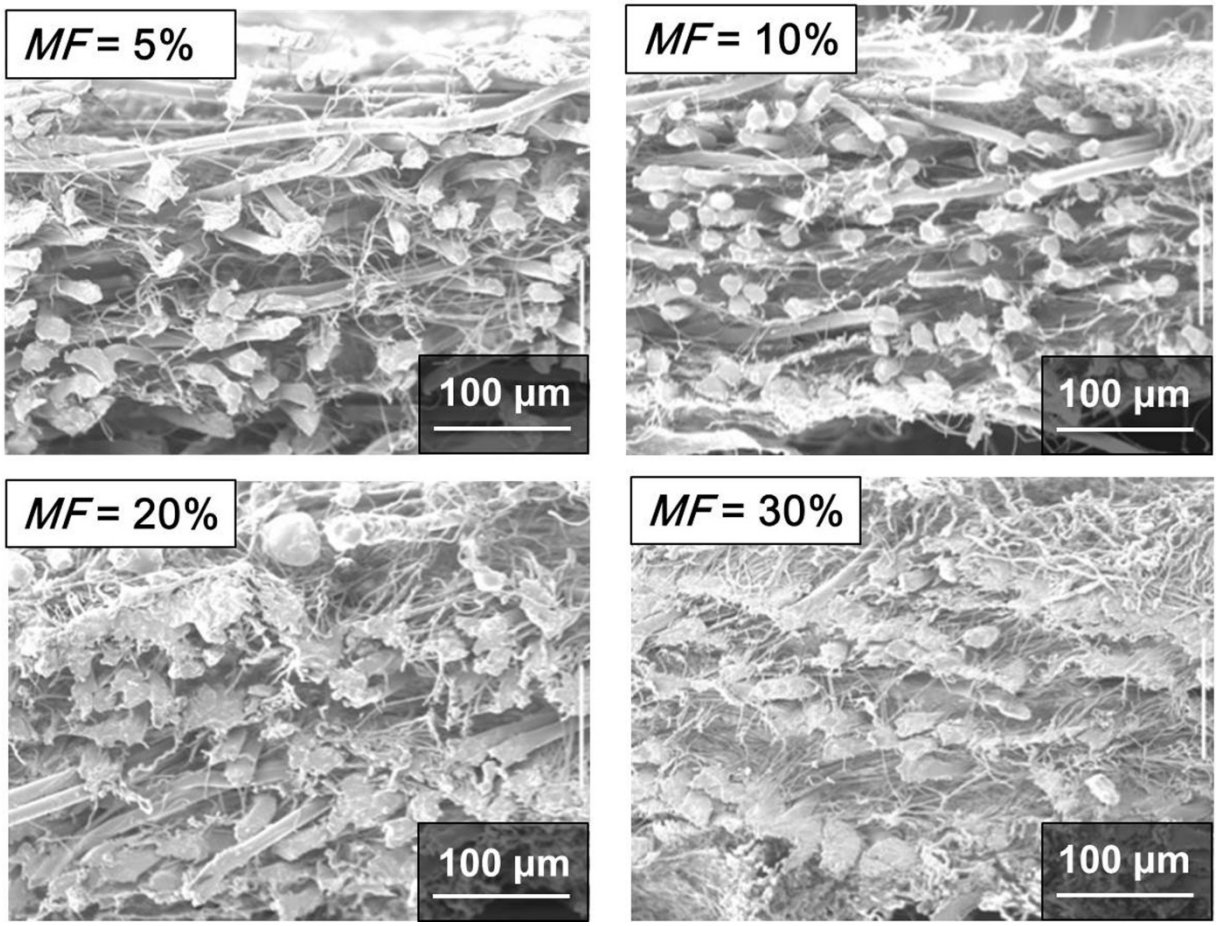

Figure 2

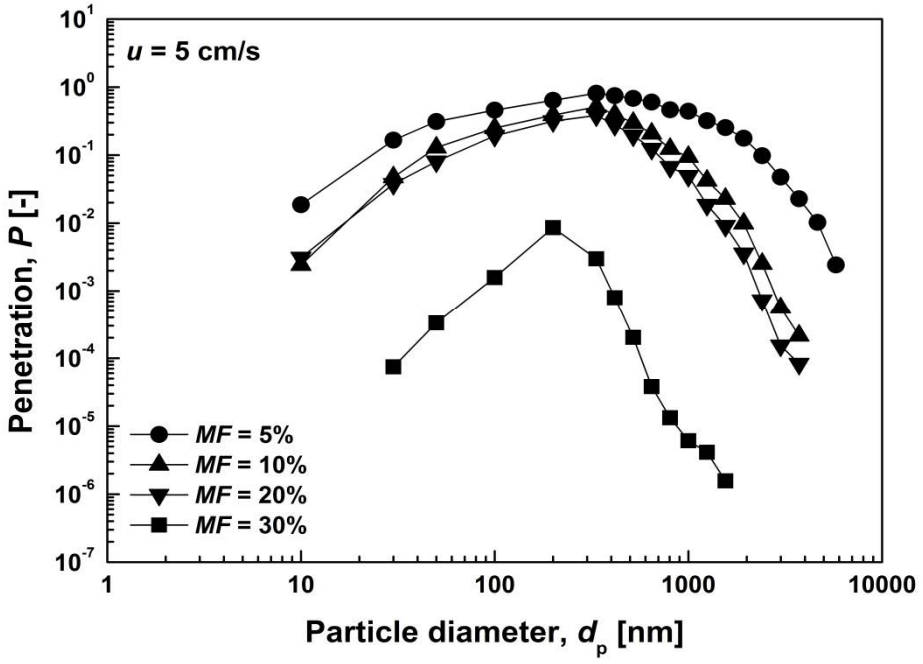
u = 5 cm/s
Penetration, P [-]
Particle diameter, d_p [nm]
MF = 5%
MF = 10%
MF = 20%
MF = 30%

(a)

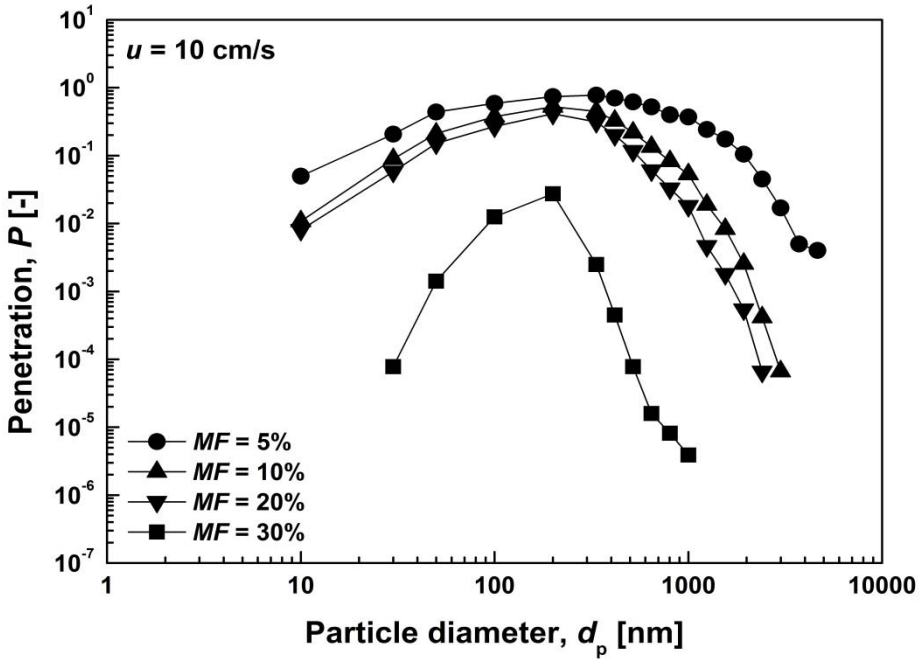
u = 10 cm/s
Penetration, P [-]
Particle diameter, d_p [nm]
MF = 5%
MF = 10%
MF = 20%
MF = 30%

(b)

Figure 3

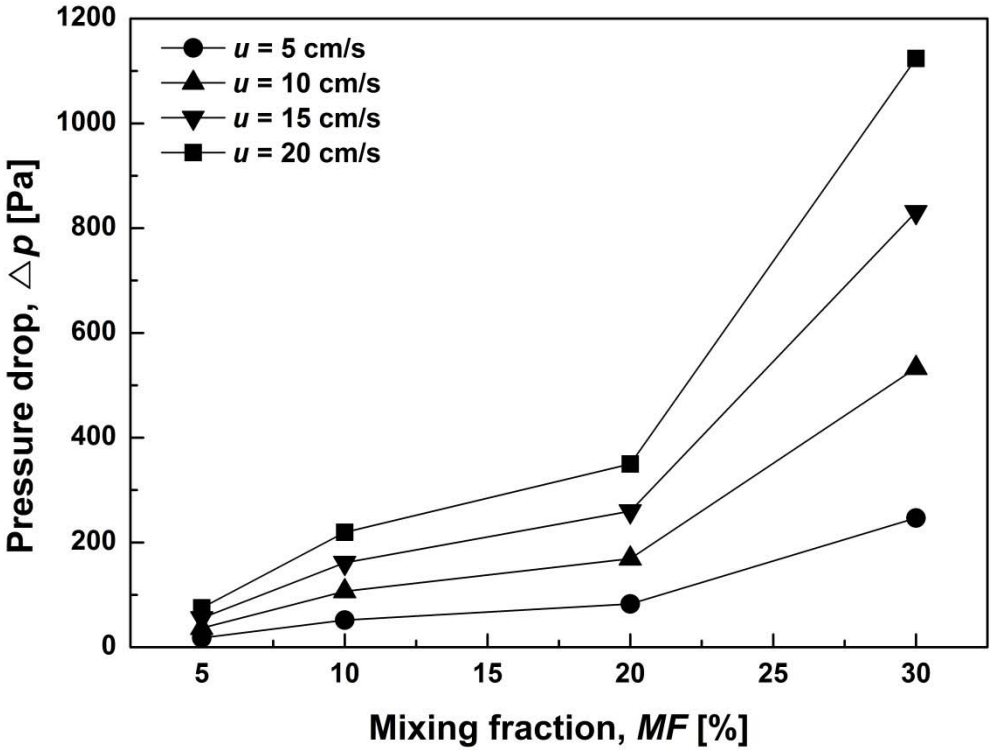
u = 5 cm/s
u = 10 cm/s
u = 15 cm/s
u = 20 cm/s
Pressure drop, △p [Pa]
Mixing fraction, MF [%]
0
200
400
600
800
1000
1200
5
10
15
20
25
30

Figure 4

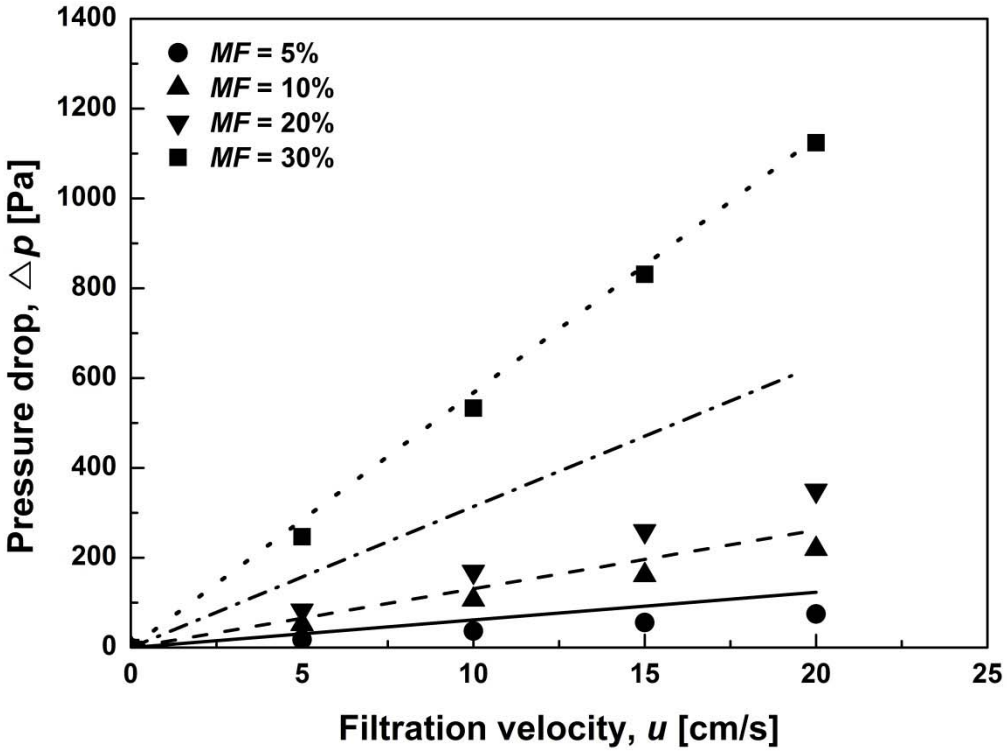
MF = 5%
MF = 10%
MF = 20%
MF = 30%
Pressure drop, △p [Pa]
Filtration velocity, u [cm/s]
0
200
400
600
800
1000
1200
1400
0
5
10
15
20
25

Figure 5

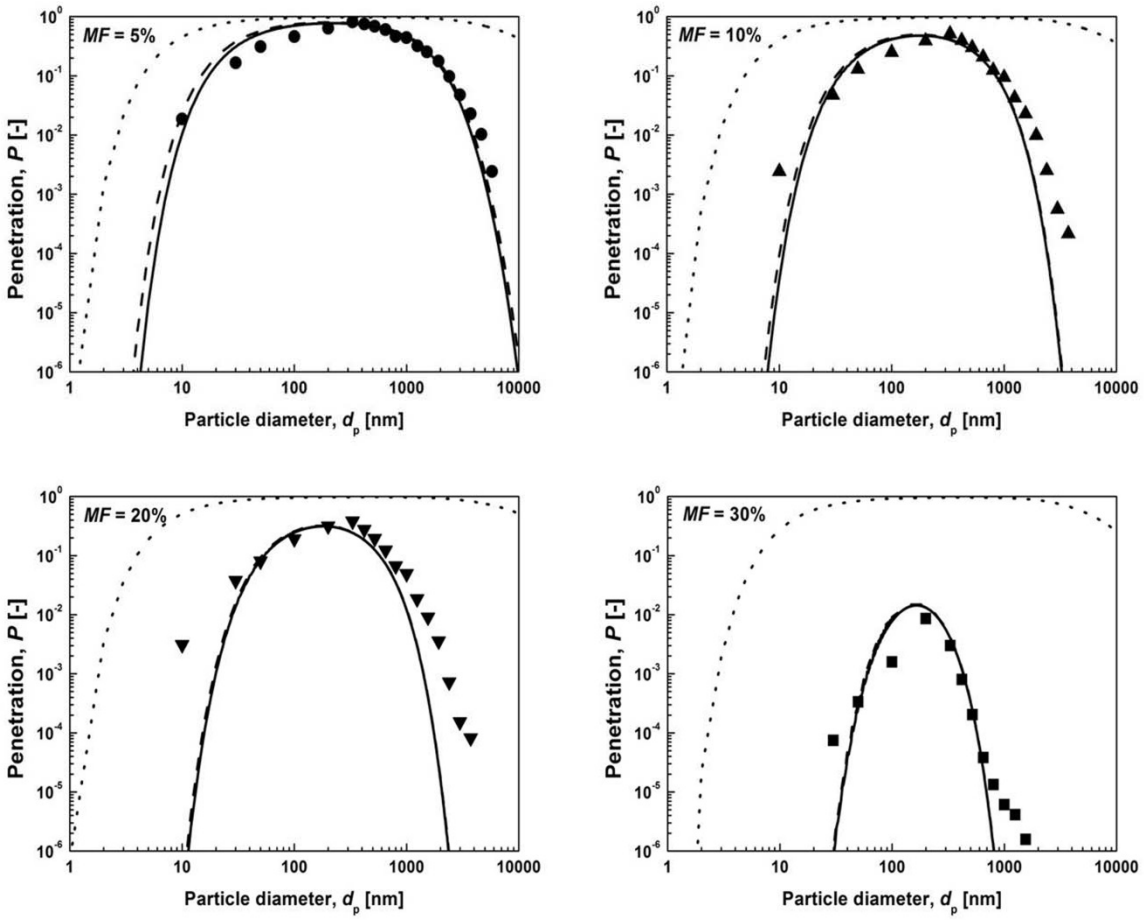

Figure 6

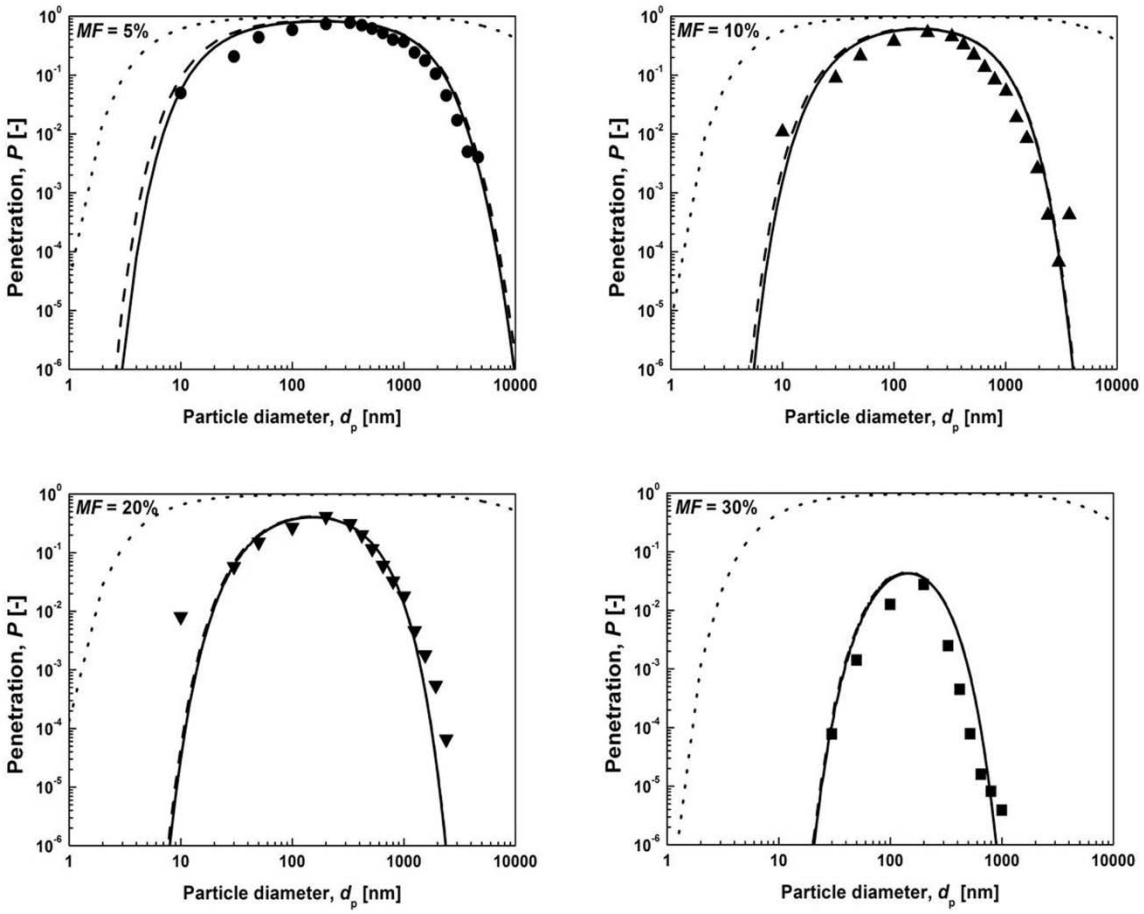
MF = 5%
MF = 10%
MF = 20%
MF = 30%
Penetration, P [-]
Particle diameter, d_p [nm]
10^0
10^-1
10^-2
10^-3
10^-4
10^-5
10^-6
1
10
100
1000
10000

Figure 7

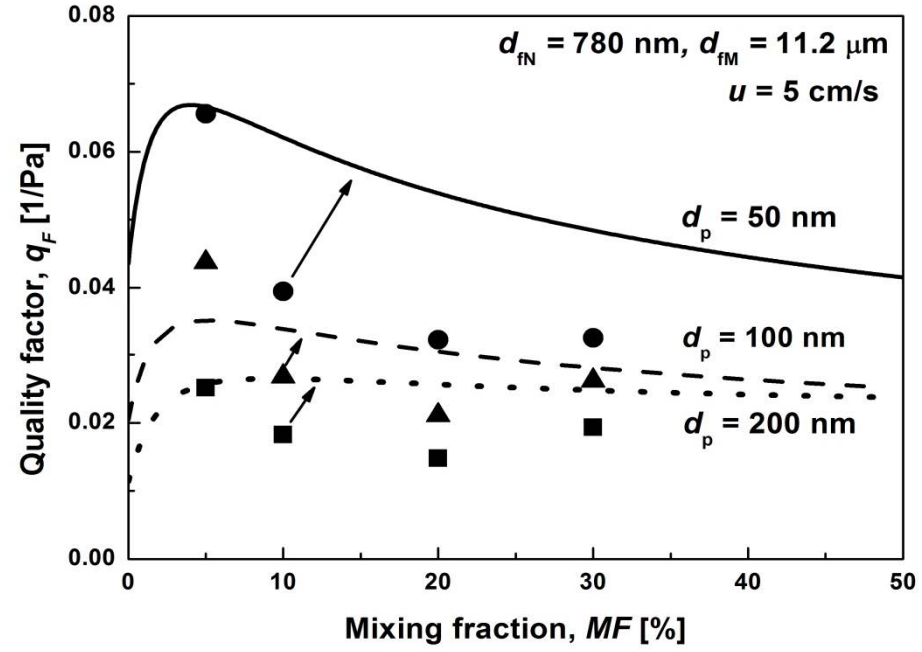
d_{fN} = 780 nm, d_{fM} = 11.2 μm
u = 5 cm/s
d_p = 50 nm
d_p = 100 nm
d_p = 200 nm
Quality factor, q_F [1/Pa]
Mixing fraction, MF [%]
0.00
0.02
0.04
0.06
0.08
0
10
20
30
40
50

(a)

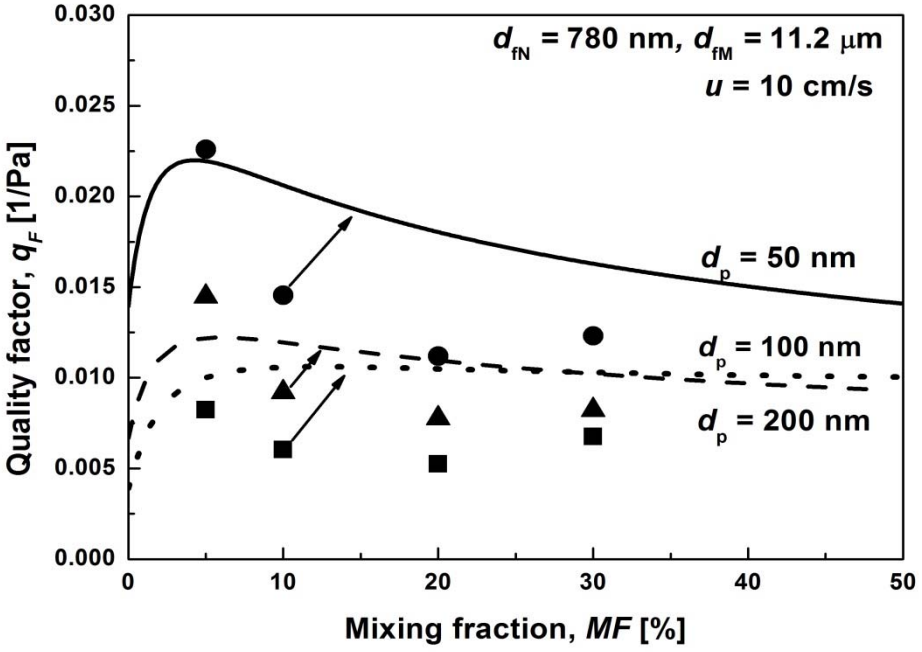
d_{fN} = 780 nm, d_{fM} = 11.2 μm
u = 10 cm/s
d_p = 50 nm
d_p = 100 nm
d_p = 200 nm
Quality factor, q_F [1/Pa]
Mixing fraction, MF [%]
0.000
0.005
0.010
0.015
0.020
0.025
0.030
0
10
20
30
40
50

(b)

Figure 8

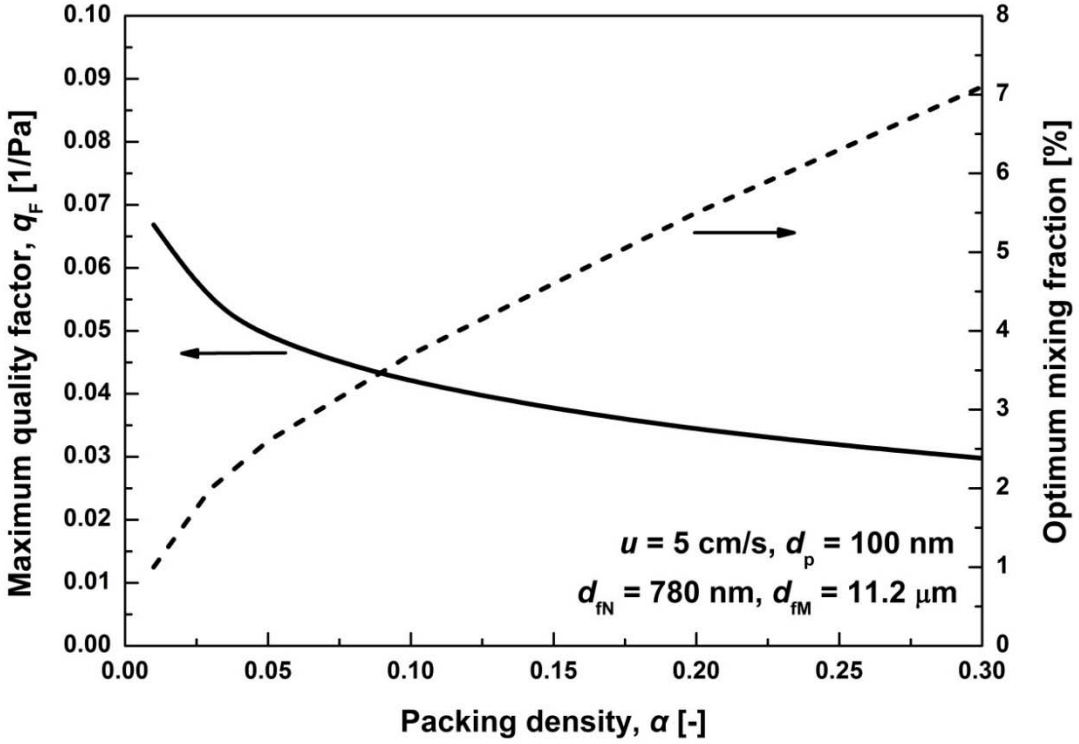
Maximum quality factor, q_F [1/Pa]
Optimum mixing fraction [%]
Packing density, α [-]
u = 5 cm/s, d_p = 100 nm
d_{fN} = 780 nm, d_{fM} = 11.2 μm
0.00
0.01
0.02
0.03
0.04
0.05
0.06
0.07
0.08
0.09
0.10
0
1
2
3
4
5
6
7
8
0.00
0.05
0.10
0.15
0.20
0.25
0.30

Figure 9

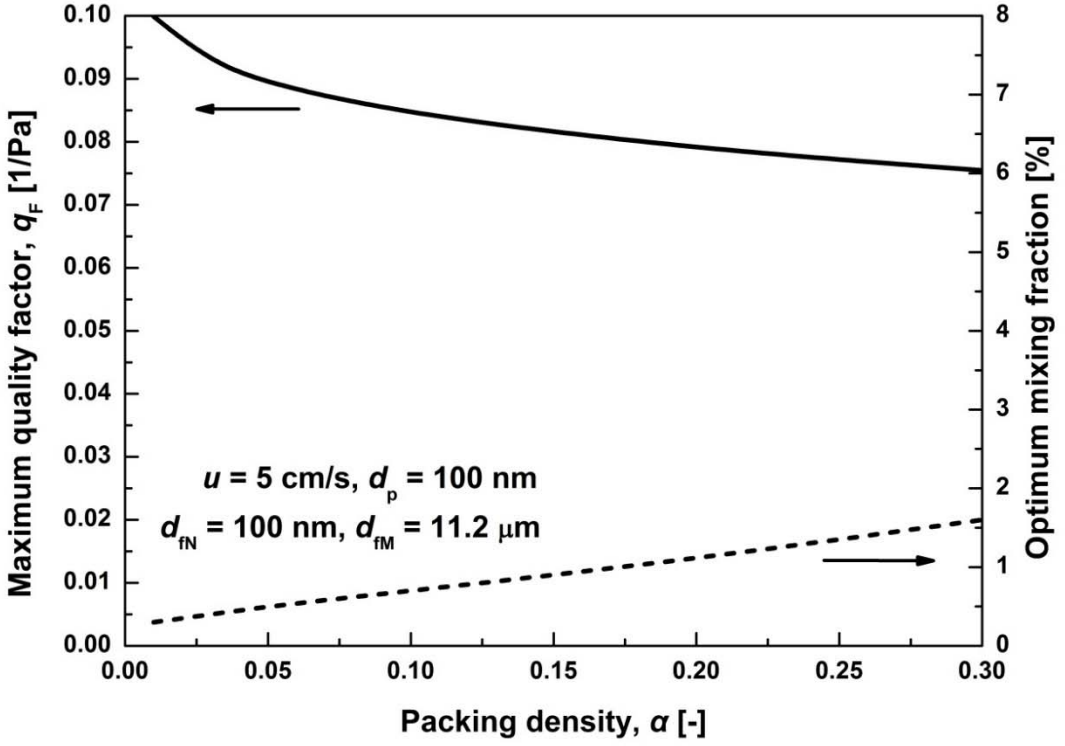
Maximum quality factor, q_F [1/Pa]
Optimum mixing fraction [%]
Packing density, α [-]
u = 5 cm/s, d_p = 100 nm
d_{fN} = 100 nm, d_{fM} = 11.2 μm
0.00
0.01
0.02
0.03
0.04
0.05
0.06
0.07
0.08
0.09
0.10
0
1
2
3
4
5
6
7
8
0.00
0.05
0.10
0.15
0.20
0.25
0.30

Figure 10